Journal of Ceramic Processing Research. Vol. 13, Special. 2, pp. s282~s285 (2012)

J O U R N A L O F
Ceramic
Processing Research

Preparation and properties of Bi-based lead-free ceramic multilayer actuators

Van-Quyet Nguyen[a], Hyoung-Su Han[a], Han-Bok Lee[a], Jong Il Yoon[b], Kyoung Kwan Ahn[b] and Jae-Shin Lee[a,*]
[a]*School of Materials science and Engineering, University of Ulsan, Republic of Korea*
[b]*School of Mechanical Engineering, University of Ulsan, Ulsan, Republic of Korea*

Lead-free ($Bi_{0.5}Na_{0.41}K_{0.09}$)$TiO_3$ (BNKT) multilayer ceramic actuators were prepared using tape-casting and screen-printing techniques. Co-firing behavior of BNKT/AgPd laminates was examined as a function of sintering temperature. It was found that co-firing induced bending and electrical properties were very sensitive to sintering condition. By optimizing sintering conditions, lead-free electrostrictive multilayer actuators with normalized strain S_{max}/E_{max} of 266 pm/V have been successfully fabricated, which is promising for lead-free actuator applications.

Key words: Multilayer actuator, Internal electrode, Thermal shrinkage, Interface.

Introduction

Piezoelectric multilayer actuators (MLAs) are widely used in applications requiring precision displacement control or high generative force, for example, optical stages, precision mechatronics, and semiconductor devices [1, 2]. Recently, lead-free piezoelectric ceramics are intensively and extensively studied to expel lead-containing PZT ceramics because there has been increasingly concerned on environmentally friendly materials in electronic and automotive industries.

Among various lead-free ceramics, (1-x) ($Bi_{1/2}Na_{1/2}$)TiO_3 - x($Bi_{1/2}K_{1/2}$)TiO_3 solid solutions (BNKTs) attract great attention due to their excellent ferroelectric and piezoelectric properties near the rhombohedral-tetragonal morphotropic phase boundary (MPB) at $0.16 \leq x \leq 0.20$ [3-6]. However, there has been little report on MLAs using BNKT-based lead-free piezoelectric ceramics even though numerous works were reported on the bulk properties of Bi-based lead-free piezoelectric ceramics. Therefore, this study aims to investigate the co-firing behavior and piezoelectric properties of BNKT/AgPd MLAs. In this work, 3 mol% Nb-doped BNKT ceramic (BNKTNb) was selected as an electrically active layer because of its large strain (S_{max}/E_{max} = 641 pm/V) in a bulk state [7].

Experiments

Powder state ($Bi_{0.5}Na_{0.41}K_{0.09}$)($Ti_{0.97}Nb_{0.03}$)$O_3$ (BNKTNb) was synthesized using a conventional solid-state reaction route starting with Bi_2O_3 (99.9%), Na_2CO_3 (99.9%), K_2CO_3 (> 99%), TiO_2 (99.9%), and Nb_2O_5 (99.9%) reagents. The powders were weighed according to the chemical formula and then ball-milled for 24 hrs in ethanol solution with zirconia balls. The slurry was dried and calcined at 850 °C for 2 hrs and then ball-milled again using the same milling media for 48 hrs. AgPd-ceramic composite pastes were prepared by adding 10 wt.% BNKTNb ceramic powders to a commercial AgPd (7 : 3) paste (SJA-73-731, Sung Jee Tech, Korea). The BNKTNb powder was first mixed with solvent and dispersant. Then, binder and plasticizer were added to the mixed slurry. The green sheets were tape-casted by a doctor blade method to a thickness of about 200 μm. The AgPd-ceramic composite paste was screen-printed on the ceramic sheet as an inner electrode, and then 14 layers of ceramics sheets were laminated by stacking and warm-pressing at 50 °C under 50 MPa for 2 min to develop good adhesion between layers. After soaking at 500 °C for 4 hrs to remove the organic additives contained in the green sheets, the samples were sintered at temperatures of 1100 - 1140 °C for 2 hrs in air. The crystal structure was analyzed using an X–ray diffractometer (XRD, RAD III, Rigaku, Japan). The surface morphology was observed with a field-emission scanning electron microscope (FE–SEM, Jeol, JSM-65OFF, Japan). The electric field-induced strain of MLAs was measured with a laser displacement measurement system (Demodulator-3700, Graphtec, Japan).

Results and discussions

A photograph of a lead-free BNKTNb MLA prepared in this study is shown in Fig. 1(a). The dimension of a specimen with 14 piezoelectric layers was about 9 mm × 7 mm × 2.2 mm. The cross-sectional SEM micrograph of a multilayered structure is shown in Fig. 1(b). It is clearly seen that the BNKTNb ceramic (dark region) and AgPd (bright region) layers are

*Corresponding author:
Tel : +82-52-259-2245
Fax: +82-52-259-1688
E-mail: jslee@ulsan.ac.kr

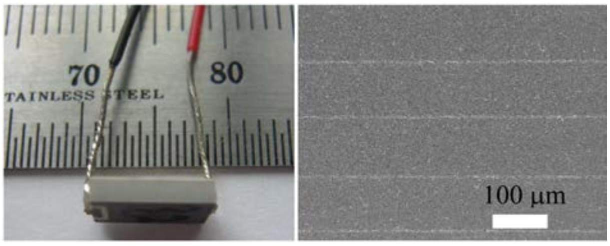

Fig. 1. (a) Photograph of a multilayer ceramic actuator. (b) Cross-sectional SEM micrograph of a BNKTNb/AgPd multilayer actuator after cofiring at 1110 °C for 2 hrs.

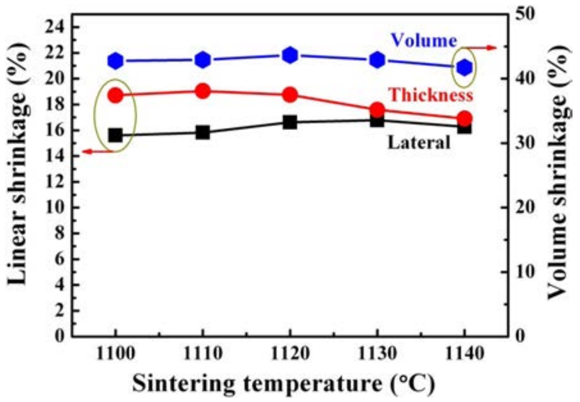

Fig. 2. Linear and volume shrinkages of the BNKTNb MLAs as a function of sintering temperature.

densely stacked with high uniformity in thicknesses. The thicknesses of ceramic and inner electrode layers are about 100 µm and 2.5 µm, respectively.

Fig. 2 shows the linear and volume shrinkage of MLAs as a function of sintering temperature (T_s). It can clearly be seen that with increasing T_s, the lateral shrinkage increases while thickness shrinkage decreases.

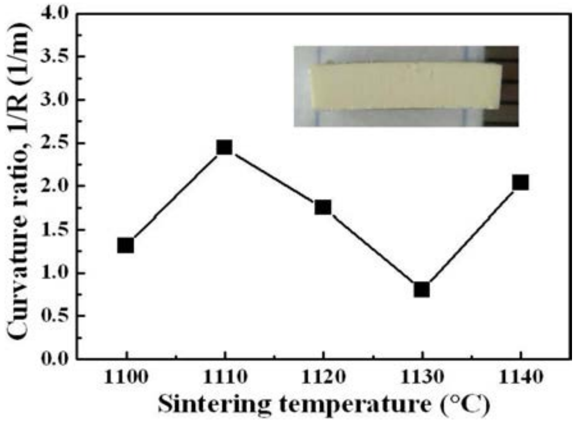

Fig. 3. Cofiring-induced deflection of a MLA as a function of sintering temperature. The photograph in the inset shows a typical bending observed in a specimen after cofiring.

In addition, the thickness shrinkage is larger than the lateral shrinkage, suggesting higher densification in metal layers due to lower melting point than that of piezoelectric ceramics. The larger shrinkage in the metal inner electrode than in the piezoelectric ceramics was experimentally confirmed in a previous study on the co-firing of lead zirconate titanate-based MLAs using a thermo-mechanical analysis [8].

After co-firing, specimens revealed a deflection as shown in the inset of Fig. 3. The co-firing-induced curvature in a sample was measured on the basis of the method proposed by Jean *et al.* [9] and the result is shown in Fig. 3(b). With increasing T_s, the curvature increased first, reached a maximum value at 1110 °C, and then decreased down to a minimum value of 0.8 m^{-1} at 1130 °C. However, the curvature increased again at 1140 °C probably due to local melting of the internal

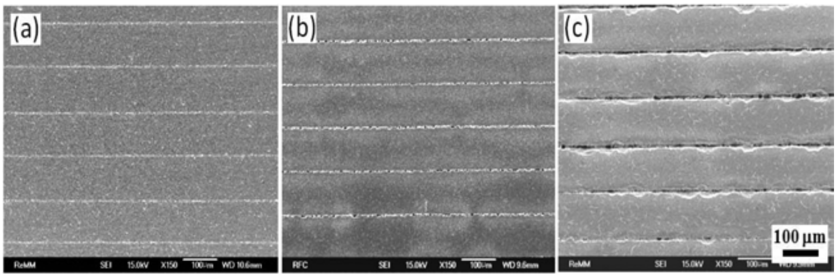

Fig. 4. Polished cross-sectional FE-SEM micrographs of BNKTNb/AgPd-ceramic multilayer composites cofired at (a) 1100 °C, (a) 1130 °C, and (b) 1140 °C, respectively.

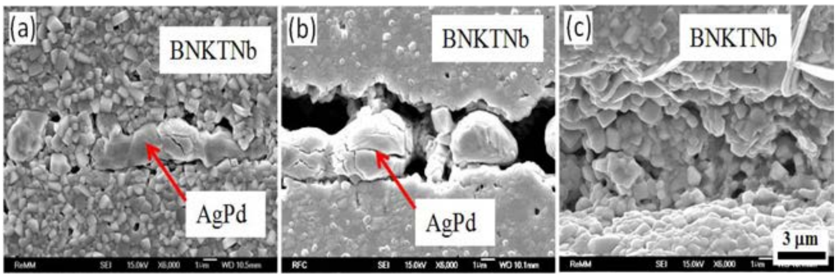

Fig. 5. Magnified micrographs of the ceramic/metal interface in the BNKTNb/AgPd-ceramic multilayer composites cofired at (a) 1100 °C, (a) 1130 °C, and (b) 1140 °C, respectively.

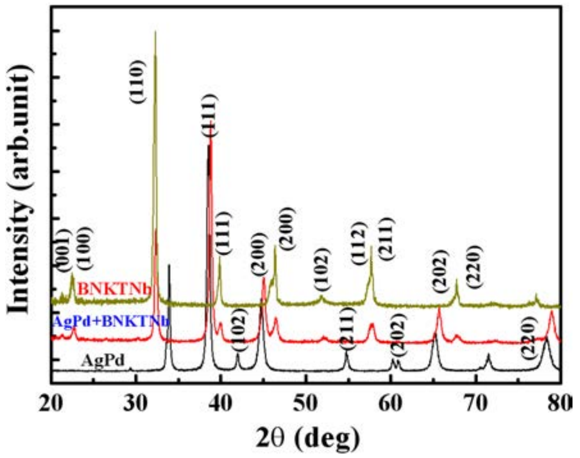

Fig. 6. The XRD patters of AgPd electrode, a pellet of 50% AgPd -50% BNKTNb mixture, and BNKTNb ceramics. The AgPd-BNKTNb composite were cofired at 1130 °C for 2 hrs.

electrode. The firing-induced bending of MLA is mainly caused by thermal mismatch between different materials. Therefore, it is believed that the thermal mismatch between two layers reached minimum when T_s = 1130 °C.

The reaction between piezoelectric and metal layers was examined by analyzing the microstructure and crystal structure. The FE-SEM micrographs of specimens sintered at 1100 °C, 1130 °C and 1140 °C were compared in Fig. 4. All specimens show good uniform ceramic layers, however, discontinuities in the electrode was observed when T_s = 1140 °C. Therefore higher magnification micrographs were taken at the metal/ceramic interface and the results were given in Fig. 5. There were two distinct changes with increasing T_s; first, the grain size of BNKTNb ceramics increased with T_s; second, inner metal layers started to coalesce into larger particles at 1130 °C and vanished at 1140 °C probably due to melting of AgPd. The melting point of AgPd (70/30) was reported to be about 1160 °C [10].

Fig. 6 presents the XRD patterns of a BNKTNb-AgPd composite that was sintered at 1130 °C for 2 hrs. The XRD patterns of pure BNKTNb and AgPd were also given for comparison. Reflections from a BNKTNb ceramic specimen correspond to those of a typical perovskite structure, while those from AgPd match to a face-centered cubic. In the case of XRD patterns of a BNKTNb-AgPd composite specimen, there is little symptom of new phases except the above two phases, indicating that there was little noticeable reaction between BNKTNb and AgPd at 1100 °C. However, careful comparison of three patterns indicates that the peak positions of both BNKTNb and AgPd in the co-fired composite were shifted toward higher angles, meaning that there were interdiffusions between two materials during sintering. In other words, silver and palladium diffuse into ceramic layers to a certain depth, and the metallic ions in the ceramic layers also tend to migrate into the AgPd internal electrode [11-13]. Because the radius of Ag^+ (0.131 nm) is close to the radii of Na^+ (0.139 nm) and K^+ (0.164 nm) [14], Ag^+ is expected to substitute onto the A-sites of BNKTNb ceramics, resulting in a decrease in the lattice parameter.

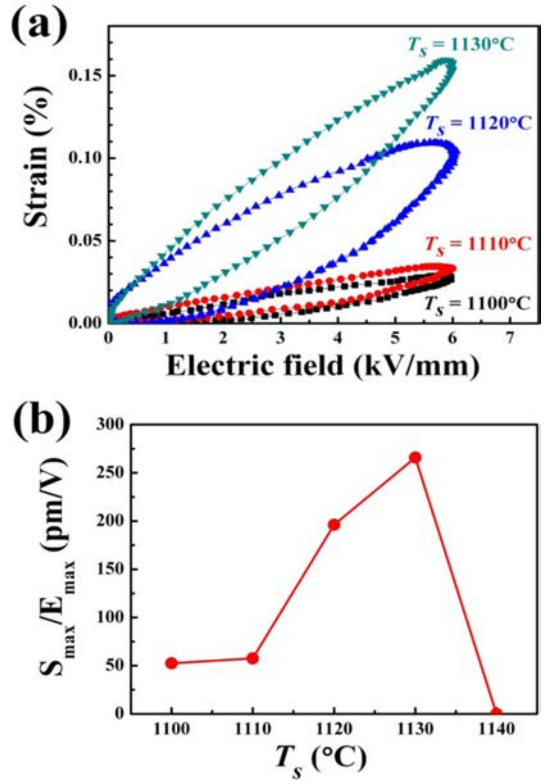

Fig. 7. Electric field-induced strain properties of lead-free BNKTNb MLAs; (a) unipolar *S-E* loops and (b) the normalized strain S_{max}/E_{max} as a function of sintering temperature.

The electric field-induced strain is the most important parameter for actuator applications. Fig. 6 displays the strain versus unipolar electric field hysteresis (*S-E*) loops and the normalized strain (S_{max}/E_{max}) as a function of T_s. The normalized strain (S_{max}/E_{max}) was enhanced up to 266 pm/V with increasing T_s up to 1130 °C, which can be attributed to the evolution of microstructure of BNKTNb ceramics as confirmed in Fig. 4. However, further increasing T_s up to 1140 °C resulted in an electrical failure of MLAs due to the melting of AgPd as observed in Fig. 4(b). It is also noted that the maximum S_{max}/E_{max} of 266 pm/V obtained in this work is much lower than that of a bulk sample (641 pm/V) reported in our previous work, which had been sintered at higher T_s of 1175 °C [7]. Such a lower S_{max}/E_{max} in the MLA might be attributed to the combined effects of the smaller grained microstructure owing to the lower T_s and the interdiffusion of elements between ceramic and metal layers during sintering even though exact understanding requests further studies.

Conclusion

Lead-free Nb-doped BNKT multilayer ceramic actuators were successfully prepared using tape-casting of green sheets and screen-printing of thick film AgPd.

The cofiring behavior and electrical properties of BNKTNb/AgPd MLAs were very sensitive to sintering temperature. With increasing T_s up to 1130 °C, which is just below the m.p. of the inner AgPd electrode, the electric field induced strain of MLAs was improved by the microstructural evolution of BNKTNb ceramics. However, the normalized strain of the MLA (266 pm/V) was found to be much lower than that of bulk BNKTNb ceramics, which seems to be caused by the combined effects of the smaller grained microstructure owing to the lower T_s and the interdiffusion of elements between ceramic and metal layers during cofiring. In order to solve this problem, further studies are thought to focus on the lowing T_s of BNKTNb ceramics as well as the modification of ceramic composition by considering interdiffusion between two materials.

Acknowledgements

This research was financially supported by the Ministry of Education, Science Technology (MEST) and National Research Foundation of Korea (NRF) through the Human Resource Training Project for Regional Innovation.

References

1. K. Uchino and S. Takahashi, Curr. Opin. Solid State Mater. Sci. 1 (1996) 698-05.
2. J. Pritchard, C.R. Bowen, and F. Lowrie, Brit. Cer. Trans. 100 (2001) 1-9.
3. A. Sasaki, T. Chiba, Y. Mamiya, and E. Otsuki, Jpn. J. Appl. Phys. 38 (1999) 5564-5567.
4. H. Ishii, H. Nagata, and T. Takenaka, Jpn. J. Appl. Phys. 40 (2001) 5660-5663.
5. K. Yoshii, Y. Hiruma, H. Nagata, and T. Takenaka, Jpn. J. Appl. Phys. 45 (2006) 4493-4496.
6. V.Q. Nguyen, H.S. Han, K.J. Kim, D.D. Dang, K.K. Ahn, and J.S. Lee, J. Alloys Compd. 511 (2012) 237-241.
7. K.N. Pham, A. Hussain, C.W. Ahn, I.W. Kim, S.J. Jeong, and J.S. Lee, Mater. Lett., 64 (2010) 2219-2222.
8. J.S. Lee, M.S. Choi, H.S. Han, Y.M. Kong, S. Kim, I.W. Kim, M.S. Kim, and S.J. Jeong, Sens. Actuators A 154 (2009) 97-102.
9. J.H. Jean, C.R. Chang, and Z.C. Chen, J. Am. Ceram. Soc. 80 [9] (1997) 2401-2406.
10. D. Schuetz, W. Krauss, J. Albering, C. Kurta, and K. Reichmann, J. Am. Ceram. Soc. 93 [4] (2010) 1142-1147.
11. R. Zuo, L. Li, and Z. Gui, Mater. Sci. Eng. 326 (2002) 202-307.
12. T. Nakamura, Y. Okana, and S. Miura, J. Mater. Sci. 33 (1998) 1091-1094.
13. Y.C. Lee, Int. J. Appl. Ceram. Technol. 7 (2010) 71-80.
14. R.D. Shannon, Acta Crystallogr. A. 32, 75 (1976) 1-767.